The binding energy of a hydrogenic impurity in self-assembled double quantum dots*

Zhang Hong(张 红)[a)†], Wang Xue(王 学)[a)], Zhao Jian-Feng(赵剑锋)[a)], and Liu Jian-Jun(刘建军)[b)]

[a)] College of Science, Hebei University of Engineering, Handan 056038, China
[b)] College of Physical Science and Information Engineering, Hebei Normal University, Shijiazhuang 050016, China

(Received 23 May 2011; revised manuscript received 29 August 2011)

The binding energy of a hydrogenic impurity in self-assembled double quantum dots is calculated via the finite-difference method. The variation in binding energy with donor position, structure parameters and external magnetic field is studied in detail. The results found are: (i) the binding energy has a complex behaviour due to coupling between the two dots; (ii) the binding energy is much larger when the donor is placed in the centre of one dot than in other positions; and (iii) the external magnetic field has different effects on the binding energy for different quantum-dot sizes or lateral confinements.

Keywords: hydrogenic impurity, double quantum dots, binding energy, magnetic field

PACS: 73.20.Hb, 73.21.La, 73.40.Kp **DOI:** 10.1088/1674-1056/20/12/127301

1. Introduction

With the rapid development in nanostructure technology, impurity doping in semiconductor materials has become important in controlling the electronic and optical properties of microelectronic devices. In recent years, using the Stranski–Krastanov growth mode, semiconductor nanostructures of different dimensions and shapes have been fabricated experimentally using molecular beam epitaxy techniques.[1−5] Meanwhile, many theoretical works[6−10] have been devoted to the study of the properties of impurity states in various confining systems. Among these theoretical works, the impurity properties of self-assembled quantum dots (QDs) are extensively studied because of their possible applications in semiconductor lasers. It is expected[11] that the QDs used as active regions in semiconductor lasers will provide low-threshold currents, high gain and improved thermal stability in the devices.

Recently, Li *et al.*[12] calculated the electronic structures and binding energy of a hydrogenic impurity in a hierarchically self-assembled GaAs/Al_xGa_{1-x}As QD in the framework of effective-mass envelope-function theory. Then they discussed the binding energy of a hydrogenic donor impurity in a rectangular parallelepiped-shaped QD in the same way, and found that the binding energies are more sensitively dependent on the applied electric field in the finite potential model, and some degeneracy is lifted when the QD is no longer cubic.[13] Perez-Merchancano *et al.*[14] discussed the binding energy of shallow hydrogenic impurities in a spherical QD under isotropic hydrostatic pressure. Qu *et al.*[15] placed the QD in an intense, high-frequency laser field. By considering the effect of an intense laser field on the binding energy, they showed a rapid decrease in the binding energy for different values of the QD radius and for both infinite and finite potential barriers, with increasing field intensity.

The coupling between the QDs should be useful in optical applications because it leads to the appearance of additional spectral lines. Liu *et al.*[16] discussed the effects of an external compressive stress on the binding energy of shallow donor impurities in cubic double QD (DQD) structures obtained by means of the variational method. Wang[17] studied the dependence of the binding energy on the donor position in DQDs using the same method, but there has some views inconsequence. Until now, there have not been any reports on the influence of the magnetic field on the binding energy of the impurity in DQDs.

In this article, we use a finite-difference method by introducing a simple model to investigate the binding energy of a hydrogenic donor impurity in self-assembled DQDs. We correct the discussion in

*Project supported by the National Natural Science Foundation of China (Grant No. 10674040), the Natural Science Foundation of Hebei Province of China (Grant No. A2011205092), and the Scientific and Technological Research and Development Projects of Handan City (Grant No. 1128120063-3).

†Corresponding author. E-mail: zhang_hong81@126.com

© 2011 Chinese Physical Society and IOP Publishing Ltd

Ref. [17], and also analyse the effects of the QD size, the lateral confinement and the external magnetic field.

2. Theory

The effective-mass Hamiltonian of a hydrogenic impurity in DQDs, in the presence of a uniform magnetic field applied in the z direction, can be written as

$$H = \frac{1}{2m_{\rm e}^*}\left(\boldsymbol{P} - \frac{e}{c}\boldsymbol{A}\right)^2 - \frac{e^2}{\varepsilon\sqrt{\rho^2+(z-z_i)^2}} + V_z(z) + V_{\rm p}(\rho), \quad (1)$$

where $m_{\rm e}^*$ and ε are the effective mass and the dielectric constant of the material of the DQDs, respectively, and $\boldsymbol{A}$ is the vector potential associated with the magnetic field. Using a cylindrical gauge, the vector potential is taken as $\boldsymbol{A} = \frac{1}{2}\boldsymbol{B}\times\boldsymbol{r}$. We consider z_i the donor position along the z axis and e the electron charge. $V_z(z)$ is the longitudinal confinement potential[18] in the Gaussian model. It can be written as

$$V_z(z) = -V_0\exp[-(z-a/2)^2/Z^2] - V_0\exp[-(z+a/2)^2/Z^2]. \quad (2)$$

Here, V_0 is the depth of the potential well, Z corresponds to the range of the longitudinal confinement, and a is the distance between the centre of the QDs. We define the barrier and spacer thicknesses by t and d, respectively, then the shape of the potential confining the charge carriers in the DQDs can be schematically displayed in Fig. 1. And the lateral potential $V_{\rm p}(\rho)$ is given by

$$V_{\rm p}(\rho) = \frac{1}{2}m_{\rm e}^*\omega_{\rm p}^2\rho^2, \quad (3)$$

in which $\omega_{\rm p}$ is a characteristic frequency associated with the intensity of the lateral confinement.

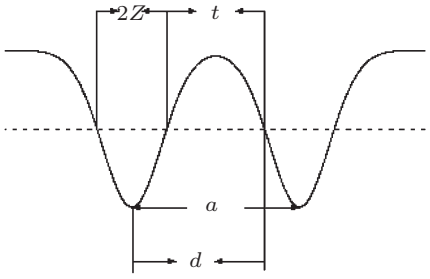


Fig. 1. Schematic diagram of the DQDs. The barrier and spacer thicknesses are denoted by t and d, respectively; a is the distance between the two dot centres.

We used the effective electron Bohr radius in the DQDs, $a_{\rm d} = \hbar^2\varepsilon/m_{\rm e}^*e^2$ as the unit of length and the effective electron Rydberg $R_{\rm d} = e^2/2\varepsilon a_{\rm d}$ as the unit of energy. In these units, the Hamiltonian (1) can be rewritten as

$$H = -\nabla^2 + \left(\frac{1}{4}\gamma_{\rm m}^2 + \gamma_{\rm p}^2\right)\rho^2 + \gamma_{\rm m}L_z - \frac{2}{\sqrt{\rho^2+(z-z_i)^2}} + V_z(z). \quad (4)$$

Here, L_z is the z component of the angular momentum operator of an electron (in units of $\hbar$); $\gamma_{\rm m}$ and $\gamma_{\rm p}$ are dimensionless measures of the magnetic field and the parabolic potential, respectively, which are defined as $\gamma_{\rm m} = e\hbar B/2m_{\rm e}^*cR_{\rm d}$ and $\gamma_{\rm p} = \hbar\omega_{\rm p}/2R_{\rm d}$. For the case of the ground state, when the eigenvalue of L_z is taken as zero, the potentials associated with the magnetic field and the lateral confinement play a similar role in the Hamiltonian. The problem has a characteristic frequency given by $\omega^2 = \frac{1}{4}\omega_{\rm m}^2 + \omega_{\rm p}^2$ ($\omega_{\rm m} = eB/m_{\rm e}^*c$), and in the absence of the impurity potential the ground-state energy can be written as

$$E_{\rm GS}^0 = \hbar\omega + E_{\rm l}, \quad (5)$$

where $E_{\rm l}$ is the electron ground state energy of the longitudinal potential.

We assume that the electron is in the ground state of transverse motion. The electron wave function for this potential can be separated in cylindrical coordinates as[19]

$$\psi(r) = \psi_\perp(\rho,\varphi)\psi_\parallel(z), \quad (6)$$

where

$$\psi_\perp(\rho,\varphi) = \frac{(\frac{1}{4}\gamma_{\rm m}^2+\gamma_{\rm p}^2)^{1/4}}{\sqrt{\pi}}\exp\left[-\frac{1}{2}\sqrt{\frac{1}{4}\gamma_{\rm m}^2+\gamma_{\rm p}^2}\rho^2\right]. \quad (7)$$

We define the operator $H_\parallel$ as the Hamiltonian for the longitudinal motion, which satisfies the equation

$$H_\parallel\psi_\parallel(z) = \int \rho{\rm d}\rho{\rm d}\varphi\psi_\perp^*(\rho,\varphi)H\psi_\perp(\rho,\varphi)\psi_\parallel(z). \quad (8)$$

Equation (8) yields

$$H_\parallel = 2\sqrt{\frac{1}{4}\gamma_{\rm m}^2+\gamma_{\rm p}^2} - \frac{\partial^2}{\partial z^2} - V_{\rm eff}(z) + V_z(z). \quad (9)$$

Here,

$$V_{\rm eff}(z) = \sqrt{2\pi}\left(\frac{1}{4}\gamma_{\rm m}^2+\gamma_{\rm p}^2\right)^{1/4} \times {\rm erfcx}\left[\left(\frac{1}{4}\gamma_{\rm m}^2+\gamma_{\rm p}^2\right)^{1/4}|z|/2\right]. \quad (10)$$

Equation (10) provides the effective potential energy of the interaction between charge carriers confined in a quasi-1D nanostructure. In Eq. (10), erfcx(t) is the exponentially scaled complementary error function. The eigenvalue problem for Hamiltonian (9) depends on only one coordinate. Therefore, it can be treated with the finite-difference method on a 1D mesh.

The ground-state binding energy $E_{\rm b}$ of the impurity is defined as the ground-state energy of the system without the impurity minus the ground-state energy with the impurity:

$$E_{\rm b} = E^0_{\rm GS} - E_{\rm min}, \tag{11}$$

where $E_{\rm min}$ is the minimum eigenvalue of $H_{\|}$ in Eq. (9).

In the next section all the numerical results have been performed for GaAs DQDs and donor impurities. The values of the parameters used in our calculations are $V_0 = 200$ meV in the Gaussian confinement, $\varepsilon = 12.5$, and $m^*_{\rm e} = 0.067m_0$, where m_0 is the free-electron mass. With this set of parameters, the effective units correspond to $a_{\rm d} = 9.87$ nm and $R_{\rm d} = 5.83$ meV.

3. Results and discussion

Figure 2 shows the binding energy of an on-centre donor in DQDs as a function of the QD size without magnetic field in Fig. 2(a), and with $B = 10$ T in Fig. 2(b) for lateral confinement $\gamma_{\rm p} = 0.3$ and $\gamma_{\rm p} = 2$. The solid, dashed and dotted curves correspond to the barrier thicknesses $t = 5$, 10 and 20 nm, respectively. From Fig. 2(a) we find that the binding energy has a maximum as the QD size increases for all the three barrier thicknesses; and as the barrier thickness reduces, the maximum moves to the side of the larger QD size. For small QD size, the difference among the binding energies of varied barrier thickness is large. As the QD size increases, the difference gradually dies away. This is because for the small QD size, the electron wave can penetrate the barrier to the other QD; the decline in penetration as the QD size increases leads to an increase in the binding energy, and ulteriorly the probability of penetration drops to zero and the binding energy reaches the maximum. Ultimately, as the QD size increases, the bondage of the donor decreases to the value of the 2D structure material. The line for barrier thickness $t = 5$ nm shows little difference from the other two. The binding energy first decreases, then increases, and at last diminishes again. This means that there is also a minimum point, which is induced by the complicated interaction between the lateral confinement, the QD size and the barrier thickness. Figure 2(b) shows the same as Fig. 2(a) but under the external magnetic field $B = 10$ T. The binding energies of the impurity have been greatly increased due to the presence of the magnetic field, and the binding energy for the barrier width $t = 5$ nm is evidently increased, even in small QDs. In contrast to Fig. 2(a), for the larger dot size, the lines still vary with different barrier thicknesses. This is because the magnetic field strengthens the coupling of the two QDs. We also find that the magnetic field has a much greater effect on the smaller lateral confinement ($\gamma = 0.3$) than on the larger ($\gamma = 2$) one, and is why it shows some crossing points for the different barrier thicknesses in Fig. 2(b).

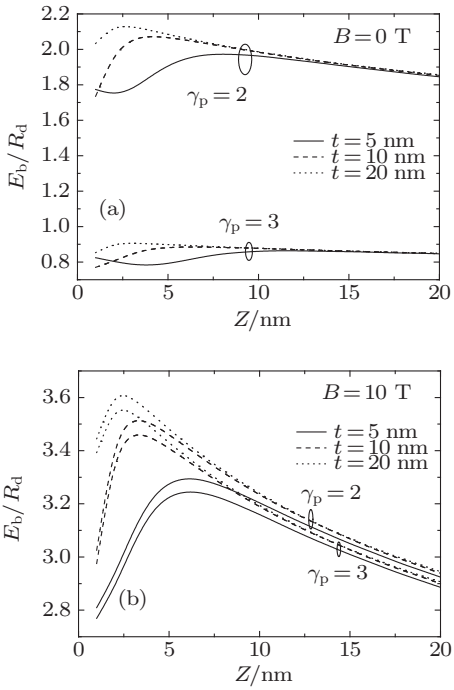


Fig. 2. The binding energy of a donor impurity at the centre of one QD as a function of the dot size for the parabolic potential for $\gamma = 0.3$ and $\gamma = 2$. The solid, dashed and dotted lines correspond to the barrier thickness being 5, 10 and 20 nm, respectively, for (a) without magnetic field and (b) with external magnetic field $B = 10$ T.

As a definition in both Ref. [17] and this article, "a" (see Fig. 1) should be larger than Z and cannot vary from zero, but the barrier thickness can. We think that the discussion of the binding energy changing as Z from zero in Ref. [17] is not suitable, so that is why here we talk about the dependence of the barrier thickness "t". Figure 3 shows the impurity binding energy as a function of the barrier thickness for

various QD sizes (z = 2, 5 and 10 nm), where the donor is placed at one dot centre. Reference [17] only gives the result for one QD size; however, we find that the variation of the binding energy with increasing barrier thickness has different behaviours for different QD sizes, as shown in Fig. 3(a). The dotted lines for the QD size z = 2 nm, which is the smallest among the three, shows that the binding energy decreases first, reaches a minimum value, then increases, and finally parallels the transverse axis. This occurs because the electron wave squeezed within the strong spatial confinement traverses the barrier region. For small barrier thickness, the electron still has strong confinement; while the barrier thickness increases, the confinement decreases. But as the barrier thickness reaches a certain value, the electron wave will barely traverse the barrier region to the other side, and therefore the binding energy begins to increase gradually. Until the electron cannot cross through the barrier, the binding energy reaches a maximum value and will not be changed whether the barrier increases or not. Then the case is like that of the single QDs. In addition, the lines for the QD sizes Z = 5 and 10 nm have no values because the spatial confinement is not strong enough to squeeze the electron out to the other side, so the binding energy increases as the barrier enhances, and this continues to a certain value. The three lines have some crossing points for small barrier thickness for the balance between the influence of QD size and barrier thickness. In the end, the barrier thickness is large enough to separate the interaction between the couple QDs, and make the DQDs change into single ones. Figure 3(b) presents the same effect of magnetic field on the binding energy as Fig. 2(b).

Figure 4 is the same as Fig. 3, but with the donor located at different places (the centre of one QD $z_i = t/2 + Z$, the edge of the barrier $z_i = t/2$ and the centre of the barrier $z_i = 0$) and the confinement of the parabolic potential γ = 2. The binding energy of the impurity at the centre of one QD as a function of the barrier thickness has been shown in Fig. 3, so we only analyse the donor placed at the edge and centre of the barrier. When the donor is located at the edge of the barrier, the binding energy for QD size Z = 2 nm and 5 nm (as the barrier thickness increases) firstly diminishes until it reaches a minimum, then increases and finally becomes a constant. For larger QD sizes Z = 10 nm, the impurity binding energy decreases monotonically as the barrier thickness increases until it reaches a minimum value. Then it does not change as the barrier thickness increases due to the weakness of the geometric confinement. Contrary to the case of the donor placed at the centre of the QD, when the binding energies are immovable, the values of the binding energy for small QD sizes are larger than those with large QD sizes because the electron is confined to just one dot space, and as the space extends the confinement weakens. In contrast to the two cases mentioned above, when the impurity is placed at the centre of the barrier, the binding energy reduces monotonously as the barrier thickness increases without a steady value.

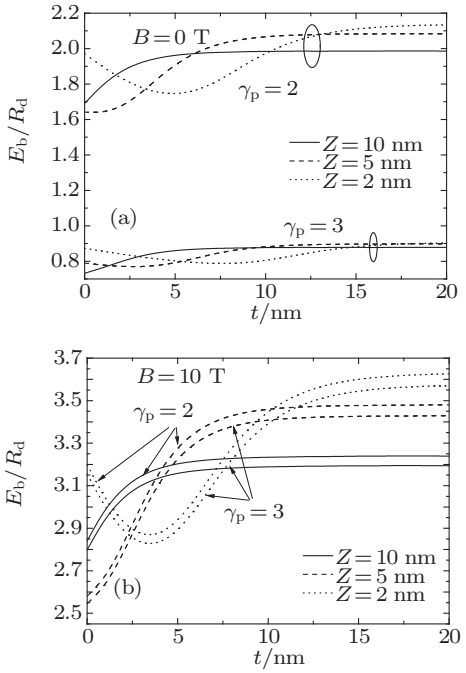


Fig. 3. The binding energy of a donor impurity at the centre of one QD as a function of barrier thickness for parabolic potential $\gamma = 0.3$ and $\gamma = 2$. The solid, dashed and dotted lines correspond to QD sizes of 10, 5, and 2 nm, respectively, (a) without magnetic field and (b) with external magnetic field B = 10 T.

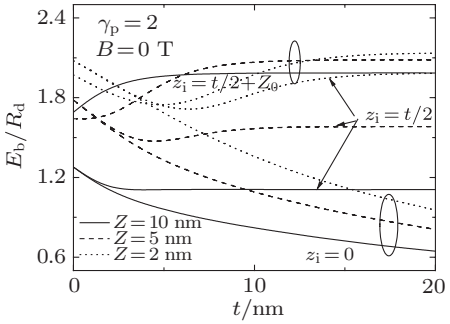


Fig. 4. The binding energy of a donor impurity as a function of the barrier thickness with the donor located at one QD centre ($z_i = t/2 + Z$), the barrier edge ($z_i = t/2$) and the barrier centre ($z_i = 0$) for QD sizes Z = 10, 5, and 2 nm.

Since the donor ion is in the barrier and the electron is in the dot space, the larger the barrier thickness the weaker the confinement.

In Fig. 5, we present the effects of lateral confinement on the impurity binding energy for variational donor position in DQDs without external field, corresponding to two barrier thicknesses of $t = 5$ and 10 nm. In the weak confinement regime, where the lateral confinement energies are lower than the binding energy of a donor in the bulk ($\gamma_{\rm p} < 1$), a linear behaviour with the variation in confinement is expected, since in this limit the lateral confinement potential can be considered as a small perturbation. For a strong lateral confinement, the binding energy is less sensitive to the increase in parabolic confining potential compared with the effect of donor position. When the donor is placed at the edge or the centre of the central barrier, the electron is restricted in the dot and can hardly leap over the barrier. That is why the binding energy is almost independent of the parabolic potential when $\gamma_{\rm p} > 5$.

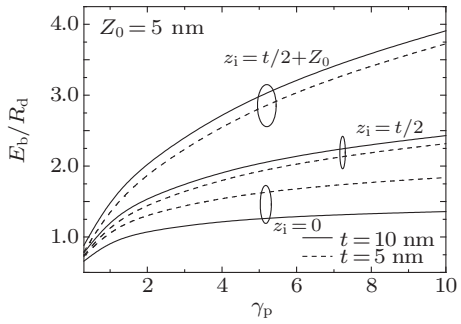


Fig. 5. The binding energy of a donor impurity in DQDs without applied magnetic field as a function of the parabolic potential $\gamma_{\rm p}$ for different locations.

4. Conclusions

In this article we correct the results in Ref. [17]. As well as the dependence of the distance between the QDs for different impurity positions, we also consider the effects of QD size, lateral potential and external magnetic field strength. The calculation method presented in this paper can be more easily compared with the variational method used to calculate how the impurity states change with the construction and the external magnetic field. Our results are useful for the application of DQDs in photoelectric and electronic devices.

References

[1] Granados D and Garcia J M 2003 *Appl. Phys. Lett.* **82** 2401
[2] Raz T, Ritter D and Bahi G. 2003 *Appl. Phys. Lett.* **82** 1706
[3] Huang S S, Niu Z C, Fang Z D, Ni H Q and Gong Z 2006 *Appl. Phys. Lett.* **89** 031921
[4] Hashimoto T, Oshima R and Okada S Y 2007 *J. Cryst. Growth* **301–302** 821
[5] Fuster D, Alen B, Gonzalez L, Gonzalez Y and Pastor J M 2007 *J. Cryst. Growth* **301–302** 705
[6] Zhang M and Ban S L 2009 *Chin. Phys.* B **18** 5437
[7] Mikhailov I D, Betancur F J, Escorcia R A and Sieera-Ortega J 2003 *Phys. Rev.* B **67** 115317
[8] An X T and Liu J J 2006 *J. Appl. Phys.* **99** 123713
[9] Brandi H S, Latgé A and Oliveira L E 2004 *Phys. Rev.* B **70** 153303
[10] Zhang M and Ban S L 2009 *Chin. Phys.* B **18** 4449
[11] Park G, Shchechin O B, Huffaher D L and Deppe D G 2000 *Appl. Phys. Lett.* **73** 3351
[12] Li S S and Xia J B 2006 *J. Appl. Phys.* **100** 083714
[13] Li S S and Xia J B 2007 *J. Appl. Phys.* **101** 093716
[14] Perez-Merchancano S T, Paredes-Gutierrez H and Silva-Valencia J 2007 *J. Phys.: Condens. Matter* **19** 026225
[15] Qu F Y, Fonseca A L A and Nunes O A C 1997 *J. Appl. Phys.* **82** 1236
[16] Liu J J, Shen M and Wang S W 2007 *J. Appl. Phys.* **101** 073703.
[17] Wang X F 2007 *Phys. Lett.* A **364** 66
[18] Szafran B, Bednarek S and Adamowski J 2001 *Phys. Rev.* B **64** 125301
[19] Szafran B, Bednarek S, Chwiej T and Adamowski J 2003 *Phys. Rev.* B **68** 045328